Real time monitoring of the quiescent suspension polymerization of methyl methacrylate in microreactors-Part 1. A kinetic study by Raman spectroscopy and evolution of droplet size

Carlos Alberto Castor Jr., Alain Pontier, Jérôme J. Durand, José Carlos Costa da Silva Pinto, Laurent Prat

Real time monitoring of the quiescent suspension polymerization of methyl methacrylate in microreactors—Part 1. A kinetic study by Raman spectroscopy and evolution of droplet size

C.A. Castor Jr.[a,*], A. Pontier[b], J. Durand[c], J.C. Pinto[a], L. Prat[b]

[a] Programa de Engenharia Química (PEQ/COPPE), Universidade Federal do Rio de Janeiro, Rio de Janeiro, 21841-972 RJ, Brazil
[b] Laboratoire de Génie Chimique (LGC UMR 5503), Université de Toulouse, INPT, ENSIACET, 4 allée Emile Monso, BP 84234, F-31432 Toulouse, France
[c] Laboratoire de Chimie de Coordination (UPR CNRS 8241), Université de Toulouse, INPT, ENSIACET, 4 allée Emile Monso-CS 44362, 31030 Toulouse, France

HIGHLIGHTS

- Experimental work on the polymerization of droplets of MMA by using microreactors.
- The reaction kinetics was monitored by Raman spectroscopy.
- Evolution of the volume of droplets during the MMA polymerization.
- Performances between the T141 and LPO initiators were compared to each other.
- It was possible to identify three stages during the suspension polymerization of MMA.

GRAPHICAL ABSTRACT

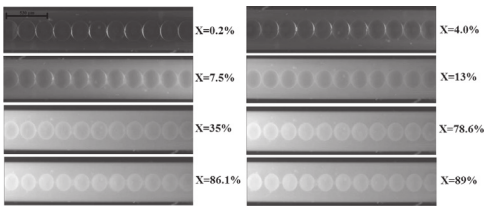

ABSTRACT

This paper presents an experimental study on the polymerization of droplets of methyl methacrylate (MMA) in quiescent state using microreactors. The reaction kinetics was monitored by Raman spectroscopy, while the images of MMA droplets image were captured by CCD (charge-coupled device) camera within a microcapillary. Different experimental recipes were proposed with commercial initiators in order to compare the system performance with two types of initiators: monofunctional and bifunctional peroxides. It is shown in this paper that the Raman technique is able to monitor the reaction kinetics at different conditions. For the first time in the open literature it was possible to identify the evolution of the monomer droplets during polymerization to high conversions ($>90\%$) in quiescent state. In addition, it was possible to identify three different stages during the polymerization reactions of MMA. Finally, it is shown that the dispersities ($\overline{M}_w/\overline{M}_n$) obtained with the bifunctional initiator were lower than 2, while the dispersities obtained with the monofunctional initiator were greater than 2.

Keywords:
Microreactors
Suspension polymerization
Raman spectroscopy
Methyl methacrylate
Kinetics
Bifunctional initiator

1. Introduction

The usage of microreactors has increased steadily in the chemical engineering field (Ehrfeld et al., 2000; Jensen, 2001; Pattekar and Kothare, 2004; Sun et al., 2008; Chang et al., 2004; Iwasaki and Yoshida, 2005; Richard et al., 2013) and also in other areas of study (Zhang et al., 2004; Salic et al., 2012; Massignani et al., 2010). The application of this technology has been proposed originally in order to allow for small-scale production and became a reality in the late 1980s and early 1990s (Benson and Ponton, 1993). In order to provide higher flexibility and allow for assessment of the capacity, safety and variability of the real process in a realistic way, microreactors should be regarded as complementary apparatuses for other existing large-scale facilities (Lerou et al., 1996; Wegeng et al., 1996). It is important

* Corresponding author.
E-mail address: carlosche@peq.coppe.ufrj.br (C.A. Castor Jr.).

to emphasize that microreactors reactors may exhibit characteristic dimensions of the order of millimeters or even smaller (Ehrfeld et al., 2000; Pattekar and Kothare, 2004; Richard et al., 2013).

Microreactors find potential use in various applications, including biocatalysis, (Fernandes, 2010), biodiesel production (Sun et al., 2008; Richard et al., 2013), heterogeneous catalysis (Kiwi-Minsker and Renken, 2005), synthesis of drugs (Kang et al., 2008), hydrogen production (Pattekar and Kothare, 2004) and polymerization processes (Bodoc et al., 2012; Bally et al., 2010). Following the general principles of the Green Chemistry, microreactors can be used to synthesize and purify organometallic compounds by atomic layer deposition (ALD) and chemical vapor deposition (CVD), allowing for safe operations and production of chemicals with higher degree of purity (Lipiecki et al., 2008, 2009).

The analysis of polymerization processes performed in microreactors is quite recent. Polymerization reactions carried out in microreactors can be divided in two main groups: homogeneous polymerizations (bulk and solution processes) (Bayer et al., 2000; Nielsen et al., 2002; Wu et al., 2004; Sotowa et al., 2004; Russum et al., 2004; Nagaki et al., 2004; Iwasaki et al., 2006) and heterogeneous polymerizations (emulsion and suspension processes) (Cabral et al., 2004; Chang et al., 2004; Nisisako et al., 2004; Jeong et al., 2005). According to the literature of heterogeneous polymerizations in microreactors, polymer samples with narrower molar mass distributions can usually be obtained in microreactors when compared to polymer samples obtained under similar conditions in macroreactors. Honda et al. (2005) produced amino acid based polymers with average molar masses controlled by the feed flow rate and with low dispersity (< 1.4). Liu et al. (2011) obtained similar results during the production of poly(butyl acrylate) (PBA) using AIBN as initiator. Particularly, dispersity decreased from 3.7 to 1.5, when microreactors were used, probably because of the higher heat exchange efficiency in the microreactor device.

Raman spectroscopy has been used in the microreactor technology, although this can still be regarded as a very new technology. Barnes et al. (2006) used the Raman technique to monitor the polymerization of benzyl methacrylate with a crosslinking agent, used for production of commercial dental composites, being the pioneer in the field. Lorber et al. (2010) monitored the polymerization of acrylic acid in aqueous solution of sodium persulfate, using the relative intensity of the vinyl double bond peak for evaluation of monomer conversion and the characteristic peak of potassium nitrate as the internal standard. Bodoc et al. (2012) applied the Raman spectroscopy to monitor the vinyl chloride polymerization in poly(vinyl alcohol) (PVA) aqueous solutions in a microreactor device. Recently, Yadav et al. (2014) applied this technique to monitor solution and miniemulsion polymerizations of styrene and butyl acrylate at different residence times.

This work presents a comprehensive study about methyl methacrylate suspension polymerizations performed in microreactors. Raman spectroscopy technique was used to monitor the kinetics of the free radical polymerization of methyl methacrylate in this heterogeneous process. Furthermore, a high speed CCD video camera was used to monitor the evolution of droplets during the suspension polymerization performed in microreactor. The polymerization setup was used to evaluate different recipes, including the use of monofunctional (lauroyl peroxide) and bifunctional (2,5-dimethyl-2,5-di(2-ethylhexanoylperoxy)hexane) initiators, in order to compare the kinetic behavior and the molar masses of the obtained of products.

2. Experimental section

2.1. Materials

All reagents were used as received. Double-deionized water was used throughout the work. The methyl methacrylate monomer stabilized with 20 ppm of hydroquinone was supplied by Sigma-Aldrich. Nitrogen gas (N_2) was supplied by Air Liquide S.A. as an ultra-pure gas and used to keep the inert atmosphere. Poly(vinyl alcohol) (PVA) with degree of hydrolysis of 89% and weight-average molar mass of 79000 g/mol was used as the suspending agent and was supplied by Sigma-Aldrich. The peroxide initiators used to perform the polymerization reactions were dilauroyl peroxide (LPO) (minimum purity of 97%, supplied by Sigma-Aldrich) and 2,5-dimethyl-2,5-di(2-ethylhexanoylperoxy)hexane (Trigonox 141) (minimum purity of 92%, supplied by Akzo Nobel). Acetone with minimum purity of 99.5% was supplied by Sigma-Aldrich and used to clean vessels and tubes. Tetrahydrofuran (THF) was used as the mobile phase for GPC analysis and was supplied by VETEC Fine Chemicals as a P.A. solvent.

2.2. Experimental apparatus

Microreactions were conducted in the experimental setup shown in Fig. 1. The components exposed to MMA, such as tubing and valves (Swagelok), were all made of stainless steel. Aqueous phase and MMA flow rates were ensured by Cetoni GmbH high pressure syringe pumps equipped with high-pressure stainless-steel syringes. The microreactor consisted of fused-silica capillary tubes inserted into a hollow metal block. The metal block was filled with silicone oil and

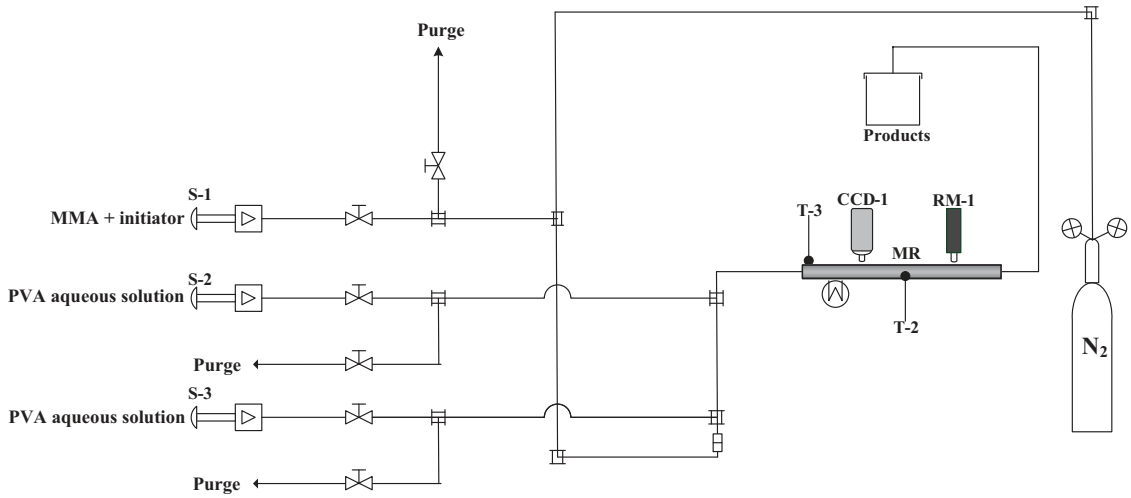

Fig. 1. Microreactor setup used for monitoring of methyl methacrylate polymerization by Raman spectroscopy and video camera techniques.

heated from inside by circulating hot oil provided by a thermal bath. At the end of the microreactor setup, a waste vessel was connected to the output line in order to collect the polymerization products.

The aqueous phase and the organic phase were put in contact with a co-axial generation device, as indicated in Fig. 2. The monomer solution (MMA+initiator) was fed through a nozzle tip of 50 μm ID (150 μm OD) fused-silica capillary tube placed inside a second capillary tube of 250 μm ID (360 μm OD). After the formation of droplets, they were pumped into a long microtube and injected into a larger fused-silica capillary of 520 μm ID (670 μm OD). A secondary aqueous flow was used to keep the desired organic holdup. The flow rates were adjusted in order to ensure that droplets would not touch the microtube walls, avoiding flow instabilities. The capillary length was equal to 60 cm.

2.3. Experimental procedure

For suspension polymerization reactions, the reaction system was first purged with nitrogen to avoid inhibition by oxygen. In all experiments, the initiator was dissolved in monomer before addition of the monomer solution into the syringe pump. Thereafter, the monomer solution was purged with nitrogen for 5 min to guarantee that the monomer was oxygen-free. The monomer solution was pumped into the microreactor in order to disperse it into the aqueous phase. The PVA was used as the surfactant agent, keeping the concentration equal to 0.3 wt.% of PVA. The flow rates used for the organic phase varied between 0.15 and 0.4 ml h^{-1} and for the aqueous phase between 1.2 and 4.0 ml h^{-1}. Once the hydrodynamic regime had been established, a first Raman spectrum was acquired at ambient temperature and used as a reference spectrum. Afterwards, the microreactor was heated to the desired temperature and the flow was stopped. Despite that, reaction was allowed to continue in the quiescent state. Experimentally, a perfect static position is difficult to obtain because of very small internal movements inside the tubing (less than 150 μm in the 2–4 h experiments); nevertheless, assumption of quiescent polymerization is certainly appropriate.

A set of MMA polymerization reactions was carried out according to the conditions shown in Table 1. The concentration of the PVA in the aqueous phase was kept constant in all reactions and equal to 0.3 wt.%. The main goal of this set of reactions was to evaluate the reaction kinetics with the help of the Raman technique and to compare the performances obtained with initiators LPO (monofunctional) and T141 (bifunctional) using conversion data and molar mass values.

The concentration of 0.5 wt.% (LPO) was taken as a reference for evaluation of active oxygen, which was similar when the concentration of bifunctional initiator (T141) was equal to 0.29 wt.%. Both concentrations lead to similar contents of active oxygen, making possible the comparison of polymer productivity obtained with these initiators. The total heating time required to heat the experimental setup from 20 °C to the reaction temperature (61–70 °C) was always close to 15–20 min.

2.4. Characterization

2.4.1. Monomer conversion

Raman spectra were obtained with a Raman spectrometer (RXN-1, Kaiser Optical System Inc.), using a near infrared laser diode (400 mW, 785 nm) as excitation source. The Raman spectra were recorded in the range of 3200–200 cm^{-1}. The microfluidic device was placed under the probe head of the spectrometer without physical contact. The distance between the optical lens and the reactor setup was approximately equal to 1.5 cm. The acquisition and processing of spectral data were performed with the proprietary software provided by iC RamanTM 4.1 *Mettler-Toledo*. The probe head was focused on the microchannel with help of a y–z barrel micrometer.

The spectra were obtained with a total integration time of 45 s (3 scans of 15 s) and the acquisition interval was equal to 60 s, using a laser with nominal output power of 200 mW. Because of the distance between the laser source and the droplets in the microcapillary, it is estimated that the laser power can be reduced by up to 40%, being influenced by several factors, including the microcapillary thickness and the aqueous phase.

2.4.2. Drops visualization

The images of the droplets during the polymerization reactions were obtained with help of an Imager Intense CCD camera (LaVision, GmbH, Germany) with maximum resolution of 1280 × 1024 pixels. The images were analyzed with the proprietary software Lavision 7.1. Details regarding the operation and applications provided by the software can be obtained from the user manual (LaVision, 2006). The camera was attached to a binocular microscope Olympus UIS2 (*BXFM Olympus microscope system*), equipped with an optical lens Olympus LMPL (65 ×) for better visualization of the internal content of the microcapillary.

Table 1
Recipes used to perform suspension polymerizations of MMA in the microreactor.

Experiment	Initiator	Temperature (°C)	Concentration (wt.%)
E1	LPO	61.0	0.500
E2	LPO	65.0	0.500
E3	LPO	67.5	0.500
E4	LPO	70.0	0.500
E5	T141	65.0	0.290
E6	T141	67.5	0.290
E7	T141	70.0	0.290
E8	T141	70.0	0.094
E9	T141	70.0	0.400

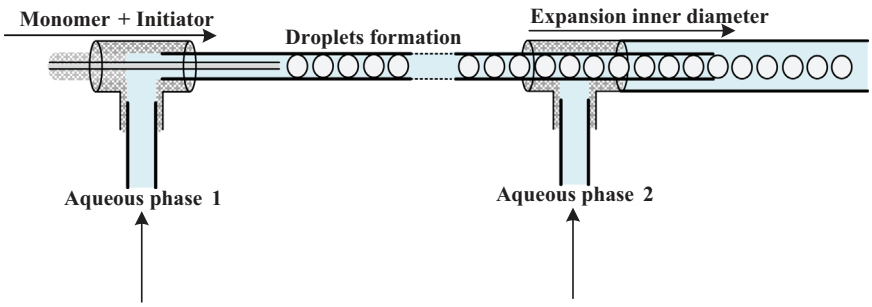

Fig. 2. Experimental apparatus for droplet formation.

2.4.3. Average molar mass

Average molar masses were determined by Gel Permeation Chromatography (GPC) with a Viscotek VE 2001 equipment, using a Viscotek VE 3580 RI refractometer detector and a series of four Phenomenex columns with porosities of 5×10^2, 10^4, 10^5 and 10^6 Å. THF was used as solvent at a flow rate of 1.0 ml min^{-1}. Calibration was performed with polystyrene standards with average molar masses ranging from 3×10^3 g mol^{-1} to 3×10^6 g mol^{-1} and checked against PMMA standards with average molar masses ranging from 3×10^5 g mol^{-1} to 3×10^6 g mol^{-1} (given the higher average molar masses of PMMA fractions) with good precision (indicating that corrections were not necessary). GPC analyses of polymer samples were performed at 40 °C and used to evaluate the evolution of average molar masses during the reaction.

3. Results and discussions

3.1. Raman monitoring procedure

The Raman spectra obtained from the reaction medium contain information about all vibrational bands related to the chemical components that constitute the system, including monomer, solvent, the aqueous phase, polymer and the microcapillary. Therefore, knowledge about the spectra of the materials that constitute the reaction medium comprises the first stage for the successful of monitoring of the process.

Fig. 3 shows the Raman spectra of methyl methacrylate and of the empty microcapillary at room temperature. As the microcapillary is made of fused silica, the baseline spectra of reagents placed inside the microcapillary are modified slightly. In order to obtain the spectrum of the pure monomer, the spectrum of the empty microcapillary was subtracted from the spectrum of the microcapillary full of MMA. After subtraction, it is possible to observe some noise near the wavelength of 2800 cm^{-1}.

One of the main features of the Raman spectroscopic technique is the high sensitivity to nonpolar bonds (McCreery, 2000; Koenig, 1999). For this reason, materials made of glass and aqueous solutions do not affect significantly the Raman spectra, although the presence of such materials can decrease the signal strength of spectral data. Thus, one must use a high-power level laser signal for efficient signal acquisition. According to Fig. 3, it can be stated that the materials that compose the microcapillary do not affect the absorption bands of the monomer MMA very significantly.

The vibrational assignments of the methyl methacrylate spectra are reported in Table 2. These vibrational bands were identified with the aid of various published works (Gulari et al., 1984; Edwards et al., 2006; Willis et al., 1969). Particular attention must be paid to the peak located at 1640 cm^{-1}. This peak represents the energy associated to the C=C stretching. As studied extensively in the literature, the monitoring of this molecular vibration during polymerization reactions can indicate the monomer consumption.

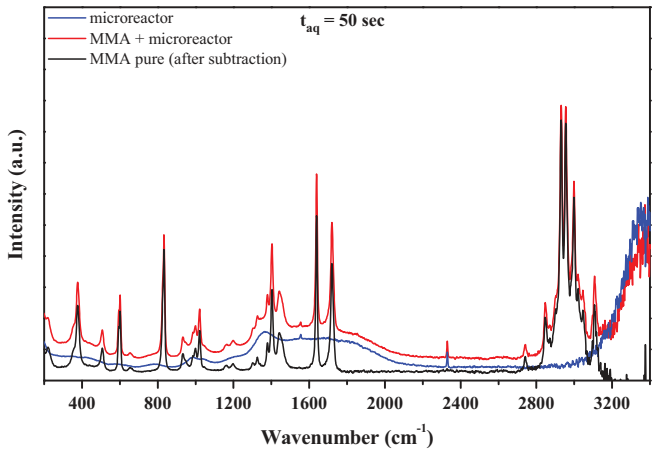

Fig. 3. Raman spectra of the empty microcapillary, microcapillary full of MMA and pure MMA at 20 °C.

Table 2
Raman bands observed in MMA spectra (Gulari et al., 1984; Edwards et al., 2006; Willis et al., 1969).

Peaks and Bands (cm^{-1})	Description of molecular vibrations
350–380	δ(C–C–C), $\delta_s(CCO)_{ip}$
507	δ(C–C–O)
602	ν(C–COO), ν_s(C–C–O) isotactic
832	ν_s(C–O–C) syndiotactic
930–1000	ν(O–C)
1021	ν_{as}(C–C)
1379	$\delta(CH_2)$ $\delta(CH_3)$ asymmetric
1403	$\delta(CH_2)$
1640	ν(C=C)
1720	ν(C=C)
2847	ν_s(C–H) from CH_2 or combinations of ν_s(O–CH)
2931	$\nu_s(CH_2)$, $\nu_s(CH_2)$ from CH_3 or O–CH_3, CH_2
3000–3100	ν(CH=C–H)

δ=deformation, ν=stretching, ip=plane, as=asymmetric, s=symmetric.

Fig. 4 shows the Raman spectrum of MMA droplets suspended in the aqueous phase within the microcapillary. From a qualitative point of view, this spectrum is identical to the spectrum of pure MMA (Fig. 3). This confirms the low sensitivity of the Raman technique to the presence of the aqueous solution, despite the presence of low amounts of PVA (0.3 wt.%).

As shown in Fig. 5, monitoring of the double bond C=C (1620–1660 cm^{-1}) during the polymerization can allow for evaluation of the MMA conversion. As expected, one can observe the decrease of the intensity of the peak C=C during the polymerization, which is correlated to the consumption of the monomer.

The analysis of the spectra shown in Fig. 5 indicates the modification of the base line due to changes of the refractive index, color, viscosity, conformation and entanglement of molecular chains and transformation of state (liquid to solid) during the polymerization. These phenomena strongly influence the intensity of the Raman signal during the polymerization (Koenig, 2001). This imposes some sort of internal calibration for quantitative monitoring of monomer consumption.

Fig. 6 shows the spectral transformation when MMA is converted into PMMA during the reaction. It can be seen that several changes take place in the Raman spectra during the course of experiment E2.

Fig. 7 shows the evolution of the area of the double bond C=C peak of MMA during experiment E2. The first 15 min of experiment E2 refers to the initial heating period and should be neglected. One can observe the continuous decrease of the peak area positioned in the region between 1620 and 1660 cm^{-1}, as expected.

As reported in the literature (Pelletier, 1999; Xie et al., 2001), during either heating or cooling one can observe changes of the intensity of the bands that comprise a particular spectrum. This effect can be associated with the more energetic state of the molecules at higher temperatures, which disfavor the secondary emission of energy of non-fundamental transitions that characterize the Raman spectrum. Moreover, the increased temperature causes changes in density and optical properties of the analyzed sample.

Xie et al. (2001) showed that the intensities of the Raman bands of metallic oxides are correlated with temperature. Thus, in order to minimize the effect of temperature while monitoring by the Raman technique, one must assure that the medium temperature is stabilized and that analyzed peaks are not very sensitive to temperature changes in the analyzed range.

The analysis of the evolution of the C═C band area shown in Fig. 7 clearly shows that the band disappears during the reaction time. The gel effect, which is a determining factor in free radical polymerization of MMA (Kalfas et al., 1993), can also be detected in the polymerization performed in the microreactor, being very well captured by the Raman technique after 100 min of reaction. After additional 20 min, one notes the relative stability of the concentration of MMA within of the droplets/particles, due to the decrease of the mobility of the macromolecular chains and the end of reaction.

In order to minimize the undesired effects of baseline variations, a commonly used procedure (Feng and Ng, 1991; Wang et al., 1992; Van et al., 2001) is the internal standardization for quantitative evaluation of conversion data. Usually, the selected reference band is a Raman band that is not modified significantly during the reaction. Particularly, the literature presents several studies (Gulari et al., 1984; Edwards et al., 2006; Feng and Ng, 1991; Hagan et al., 2009; Chu and Lee, 1984) regarding the monitoring of MMA reactions. From the literature, it can be observed that there is no consensus concerning the choice of the internal reference during the MMA polymerization. For the suspension polymerization of MMA in microreactors, this study adopted as the internal reference the region positioned between 570 and 630 cm^{-1}, according to the results shown in Fig. 8. For calculation of conversion during the MMA polymerization, the peak area of the C═C vibration (1640 cm^{-1}) was normalized with

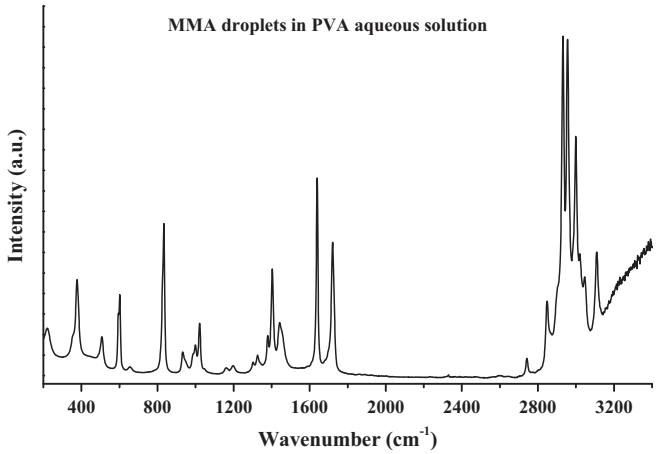

Fig. 4. Raman spectrum of MMA droplets dispersed in the PVA aqueous solution at 25 °C inside the microreactor.

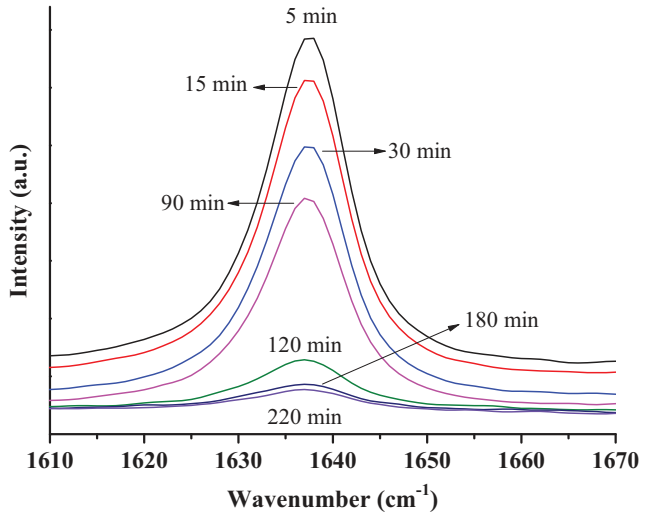

Fig. 5. Evolution of the intensity of the Raman peak at 1640 cm^{-1} (experiment E2).

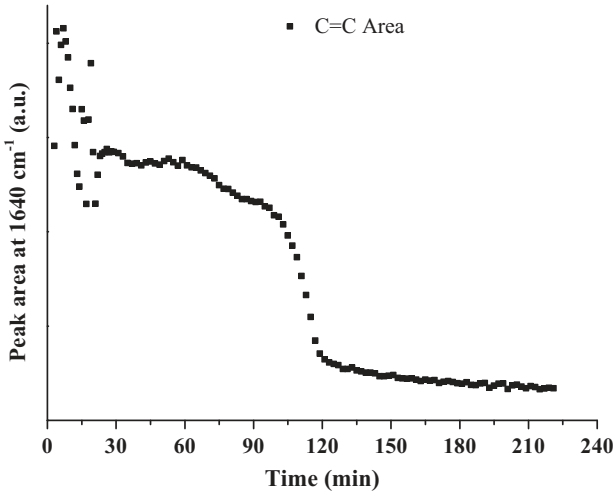

Fig. 7. Evolution of the peak area of the C═C bond during the suspension polymerization of MMA in experiment E2.

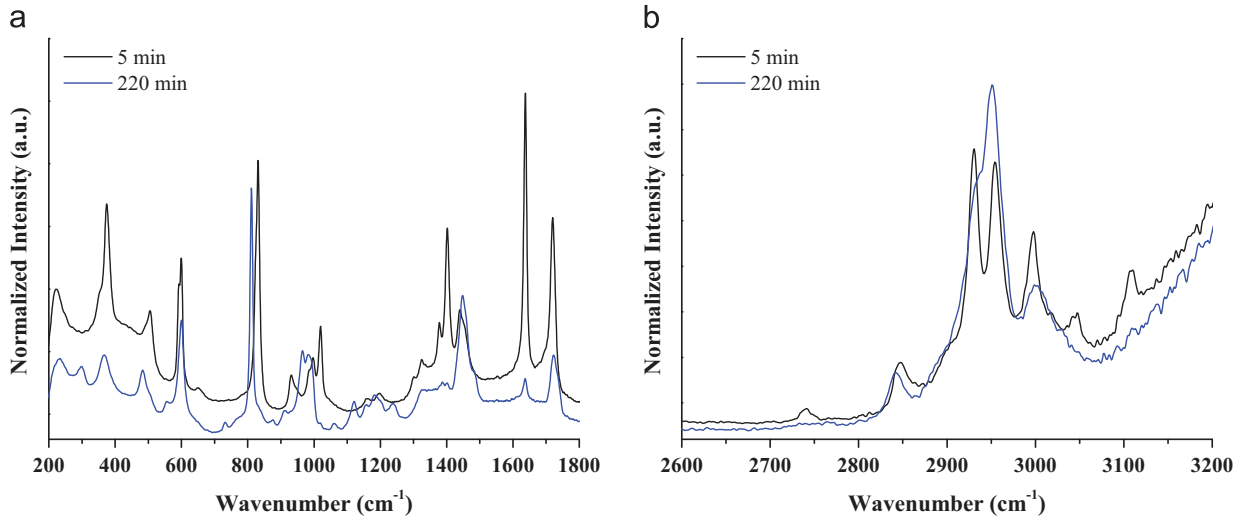

Fig. 6. Raman spectra of MMA (beginning) and PMMA (end of reaction) droplets inside the microcapillary. (a) 200–1800 cm^{-1} and (b) 2600–3200 cm^{-1}.

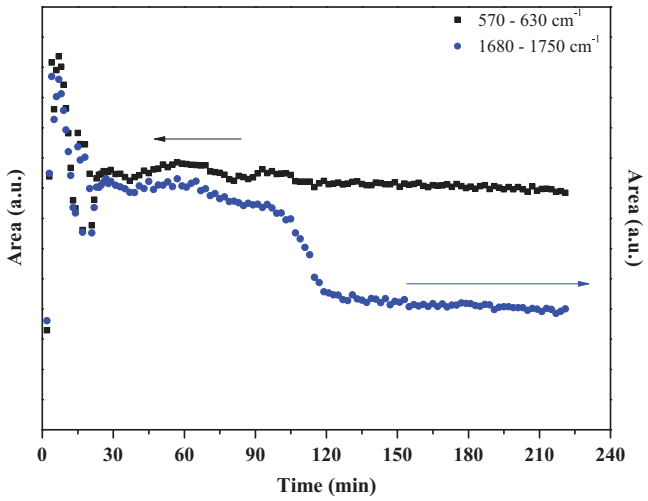

Fig. 8. Evolution of the peak areas of the carbonyl (1680–1750 cm^{-1}) and ester groups (570–630 cm^{-1}) during the experiment E2.

respect to the ester group vibration (600 cm^{-1}), according to the following equation:

$$X(t)\% = \left(1 - \frac{[m]_t}{[m]_0}\right) \times 100 = \left(1 - \frac{\frac{[C{=}C](t)}{[A_r](t)}}{\frac{[C{=}C](t_0)}{[A_r](t_0)}}\right) \times 100 \quad (1)$$

where $[C{=}C](t_0)$ is the band area corresponding to the wavelength of the double bond at the beginning of reaction, $[A_r](t_0)$ is the band area corresponding to the wavelength of the ester group at the beginning of reaction, $[C{=}C](t)$ is the band area corresponding to the wavelength of the double bond at time t and $[A_r](t)$ is the band area corresponding to the wavelength of the ester group at time t. Based on Eq. (1), one can obtain the conversion data depicted in Fig. 9.

3.2. Suspension polymerization reactions

Polymerization kinetics: Fig. 10 shows the effect of temperature on the kinetics of MMA suspension polymerizations carried out with the monofunctional initiator LPO (0.5 wt.%). The increase of the polymerization rates is observed when the reaction temperature is increased, as expected. The increase of temperature also influences the onset of the gel effect, which exerts an important influence on the polymerization of methyl methacrylate. When the gel effect takes place, a large amount of heat is released, since the polymerization is a highly exothermic process. As the reaction mixture is highly viscous, it can be difficult to remove the heat released by reaction. However, due to the high surface/volume ratio of microreactors, the temperature control problem is much less important in microreactors than in macroreactors. It is important to emphasize that the onset of the gel-effect was defined as the conversion where the second-derivative of the dynamic trajectory became positive, after the initial linear region.

In all reactions discussed here, the glass effect could also be detected. This effect is predominant at high conversions and occurs when the reaction temperature becomes smaller than the glass transition temperature (T_g) of the polymer solution. In our case, the T_g of PMMA is close to 105 °C (Brandrup et al., 1999). At very high conversions, the reduction of mobility of monomer molecules in a highly viscous medium causes the reduction of reaction rates, decreasing the monomer consumption rates and eventually causing the interruption of the polymerization.

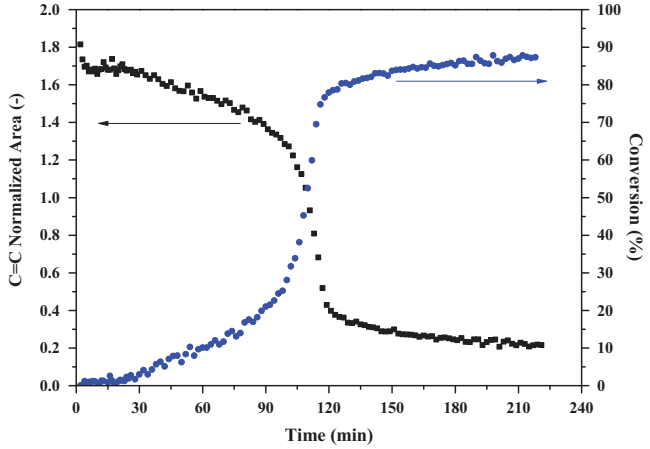

Fig. 9. Evolution of normalized area of the peak C=C relative to the ester group and MMA conversions in experiment E2.

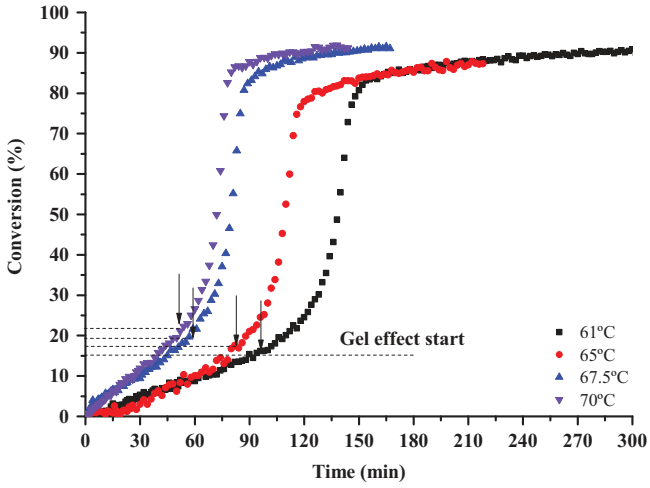

Fig. 10. Conversion data of MMA suspension polymerizations performed with 0.5 wt.% of LPO at different temperatures.

Fig. 11 compares our data to those obtained independently and published in the literature (Jahanzad, 2004), in order to evaluate the ability of the proposed Raman monitoring technique applied in the present work. Jahanzad (2004) performed MMA suspension polymerizations in a stirred tank reactor (1.0 L) at the same temperature, using gravimetric analyses to calculate the monomer conversion. Furthermore, Jahanzad (2004) performed the reactions with the same initiator (LPO), but using a concentration of 1.0 wt.%

The dynamic trajectories presented in Fig. 11 are very similar. However, as expected, the use of higher initiator concentration leads to higher reactions rates (Odian, 2004). The initial rates of polymerization can be calculated as the slopes of the initial linear regions. Based on this simple calculation, it is possible to conclude that Jahanzad (2004) obtained rates that were 70% higher than the ones obtained here, similar to the expected 40% increase predicted by the classical free-radical polymerization model. Therefore, it can be concluded that the proposed monitoring scheme is reliable and compatible with previously published data.

Average molar masses are shown in Table 3 as functions of reaction temperature for reactions performed with the monofunctional initiator LPO. As expected $\overline{M}_w$ and Đ values decrease with the increasing temperature, due to the higher sensitivity of rates of termination and transfer to monomer to modification of the reaction temperature.

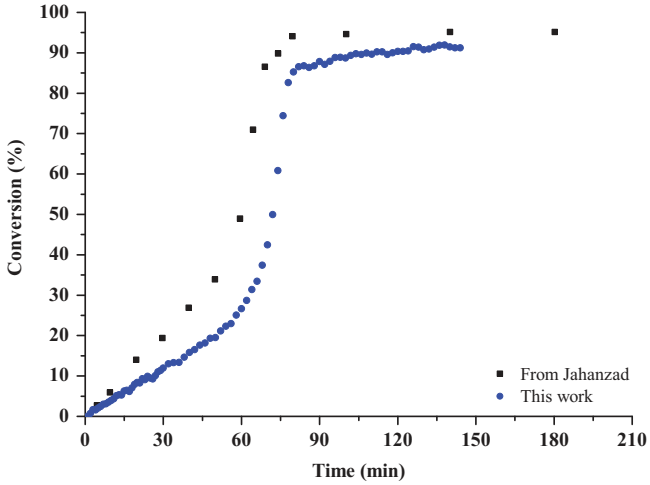

Fig. 11. Conversion data obtained in the present work and published in the literature (Jahanzad, 2004) for MMA suspension polymerizations performed with LPO at 70 °C.

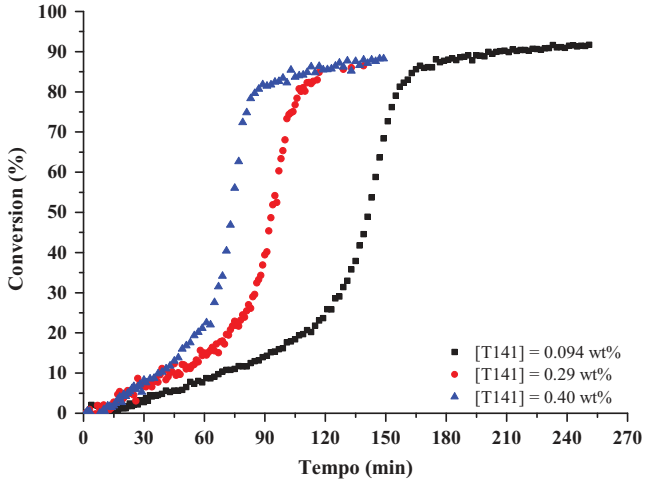

Fig. 12. Conversion data for MMA suspension polymerizations performed at 70 °C at different concentrations of initiator T141.

Table 3
Average molar masses obtained at different temperatures in reactions performed with LPO.

Temperature (°C)	$\overline{M}_w$ (kg/mol)	$\overline{M}_n$ (kg/mol)	Đ (–)
65	932,000	309,000	3.02
67.5	710,000	332,000	2.14
70	539,000	264,000	2.04

Fig. 12 shows the effect of the initiator concentration of T141 on monomer conversion. As expected, one can observe the increase of both the monomer conversions and the reaction rates with the initiator concentration. Once more, variations of the initial reaction rates were in accordance with the classical free-radical polymerization model. It is important emphasize that no studies are available in the literature regarding the use of the bifunctional initiator T141 in the suspension polymerization of methyl methacrylate. Apparently, the only work concerning the use of initiator T141 in MMA polymerizations studies the bulk polymerization of MMA in a dilatometric device (Sheng et al., 2005). These authors investigated the effects of the initiator concentration and temperature on the polymerization rate as well as the efficiency of the bifunctional initiator T141. Sheng et al. (2005) maintained the monomer conversion always below 10% to study the efficiency and the activation energy of this initiator in the initial stages of the polymerization of MMA. The efficiency of T141 was experimentally determined and found to be equal to 0.43 ± 0.02, decreasing with the increasing initiator concentration.

Keeping constant the concentration of the initiator T141 (0.29 wt.%), the reaction temperature was varied from 65 to 70 °C and conversion data were recorded, as shown in Fig. 13. As expected and observed in the case of the LPO initiator (10), higher monomer conversions were obtained when the temperature was increased.

The average molar masses of the polymer product were obtained as functions of the reaction temperature when reactions were performed with the bifunctional initiator T141, as shown in Table 4. Once more, it can be noted that the increase of temperature caused the decrease of the average molar masses and its dispersities. Similar effects were also observed in the bulk polymerization of styrene (Cavin et al., 2000) (80–110 °C) when the same initiator was employed. However, average molar masses and its dispersities obtained with the bifunctional initiator were less

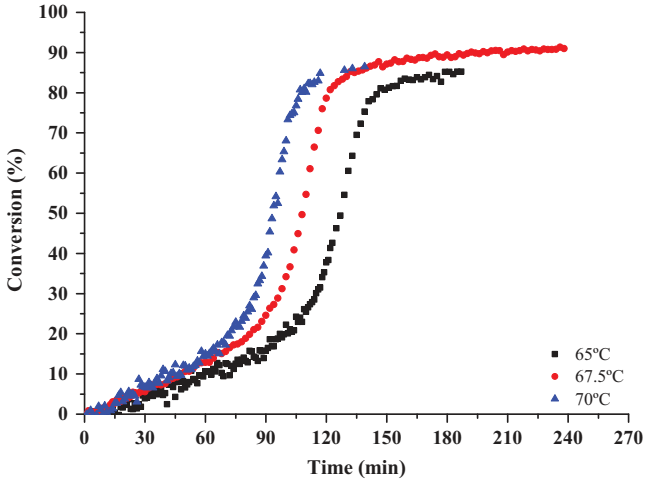

Fig. 13. Conversion data for MMA suspension polymerizations performed with the initiator T141 (0.29 wt.%) with different temperatures.

Table 4
Average molar masses obtained at different reaction temperatures reactions with T141.

Temperature	$\overline{M}_w$ (kg/mol)	$\overline{M}_n$ (kg/mol)	Đ (–)
65	995,000	536,000	1.86
70	909,000	524,000	1.73

sensitive to temperatures than observed with the monofunctional initiator.

Fig. 14 compares monomer conversions obtained when initiators LPO and T141 were used, clearly indicating that LPO leads to higher reaction rates than T141. This observation can be explained in terms of the decomposition rates of both initiators (T141 and LPO), whose values are shown in Table 5 in terms of half-life times. As the LPO has a half-life about 2.6 times lower than the initiator T141 at reaction temperatures (65, 67.5 or 70 °C), the LPO is consumed faster, resulting in higher MMA conversions. Note that for higher temperatures, conversion differences increase, suggesting the increase of the reactivity of LPO in relation to T141 in the analyzed temperature range.

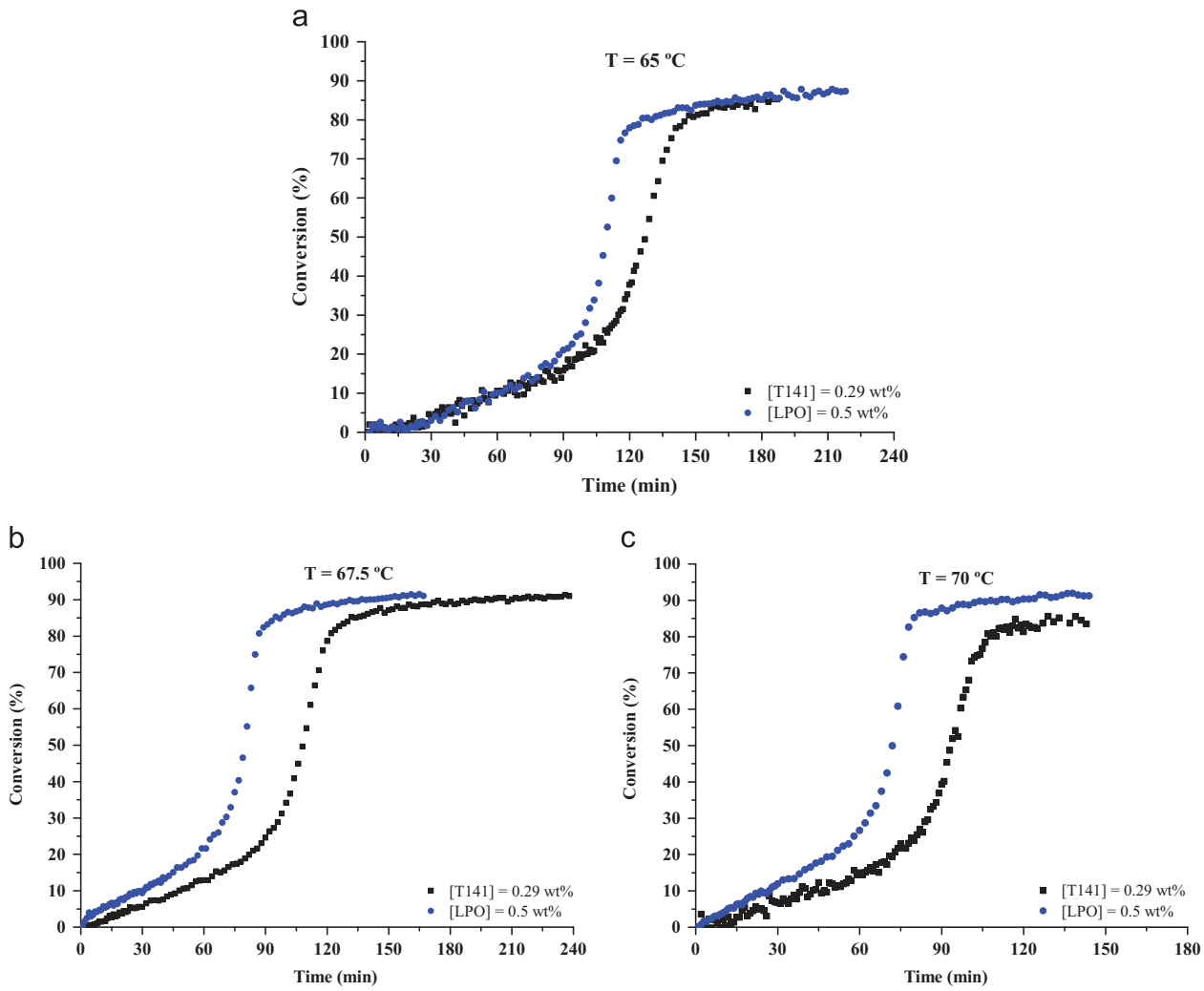

Fig. 14. Monomer conversions when the initiators LPO and T141 were used to perform the polymerization with the same concentration of active oxygen. (a) 65 °C. (b) 67.5 °C. (c) 70 °C.

Table 5
Half-life times at different temperatures for LPO and T141 (Nobel, 2008).

Initiator	Temperature (°C)	Half-life (h)
LPO	65	5.6
T141		14.5
LPO	67.5	4.0
T141		10.3
LPO	70	2.9
T141		7.4

Nevertheless, when both LPO and T141 initiators were compared for similar half-life times, higher rates of reaction were obtained with the bifunctional initiator. Fig. 15 shows that the initiator T141 leads to higher reaction rates, when compared to LPO at temperatures where both initiators present the same half-life time for similar concentrations of active oxygen; in other words, similar decomposition rates ($k_{d_{LPO}} = 2.0 \times 10^{-5}\ s^{-1}$ and $k_{d_{T141}} = 1.9 \times 10^{-5}\ s^{-1}$). Under these conditions, the kinetics of the polymerization of MMA is controlled by the kinetic rate constants, since the higher temperatures used with T141 results in higher values of the propagation rate constant, which can explain the highest reaction rates, when compared to results obtained with the initiator LPO.

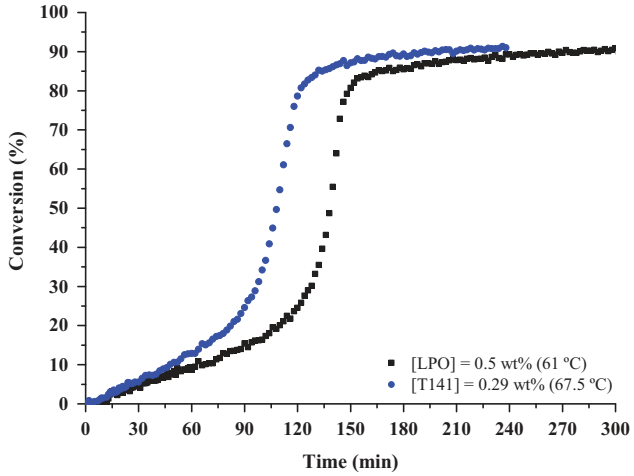

Fig. 15. Monomer conversions obtained with the monofunctional (LPO) and bifunctional (T141) initiators at similar half-life times ($t_{1/2} \approx 10$ h).

According to the classical free radical polymerization literature (Yoon and Choi, 1992; Benbachir and Benjelloun, 2001), one of the main advantages of using multifunctional initiators is the ability to simultaneously increase the average molar masses and the reaction

rates when compared to monofunctional initiators, as also observed in the present work for the MMA suspension polymerization performed in microreactors, as shown in Fig. 15 and Table 6.

Interestingly, the work by Scorah et al. (2004) did not show the increase of the average molar mass produced by bulk polymerization with the tetrafunctional initiator 2,2 bis(4,4-di-(tert-butyl-peroxy-cyclohexyl)propane) (JWEB), when compared to the product obtained with the monofunctional initiator *tert-Butylperoxy 2-ethylhexyl carbonate* (TBEC) at the elevated temperature range 90–110 °C. This particular advantage of using multifunctional initiators was also not observed either during in the bulk polymerization of butyl acrylate and vinyl acetate (Scorah et al., 2006). In these cases, transfer to monomer and to polymer seem to dominate the growth of the macromolecular chains, making the final molecular architecture of the produced polymer less sensitive to the functionality of the initiator.

3.3. Monitoring of droplets/particles volume

As reactions were conducted with the droplets dispersed in the aqueous phase inside the microcapillary in quiescent state, the effects of agitation were removed. This means that the break-up and coalescence phenomena were not present either. Fig. 16 shows the evolution of the droplets as a function of the monomer conversion, as obtained by the CCD camera in experiment E6.

In general, one can observe visually the volume contraction of the droplets/particles throughout the reaction. This result is expected due to the inherent characteristics of the polymeric material, as polymer densities are higher than monomer densities. In theory, the increase of the density is the major cause for the decrease of the size of the polymer particles, since the MMA density is equal to $\rho_{mma}(20\ ^\circ C)=$ 943.5 kg/m^3 and the PMMA density is $\rho_{pmma}(70\ ^\circ C)=1152.8$ kg/m^3 (Brandrup et al., 1999).

Table 6
Average molar masses obtained with different initiators.

Initiator	Temperature (°C)	$\overline{M}_w$ (kg/mol)	$\overline{M}_n$ (kg/mol)	Đ (–)
LPO	65	932,000	309,000	3.02
T141	65	995,000	536,000	1.86
LPO	70	539,000	264,000	2.04
T141	70	909,000	524,000	1.73

One can also observe significant changes inside the droplets during the polymerization of MMA, mainly after 13% of conversion. Between 0 and 5% of conversion no significant changes were observed within the droplets. After 5% of reaction, one can observe the gradual increase of the opacity, characterized by the increase of the polymer concentration and the progressive change of the optical properties of the material. Despite the total solubility of PMMA in its monomer, it can be noted that the growth of the polymeric chains significantly modifies the refractive index of the particles, mainly after 15% conversion. After 35%, changes of the opacity can be seen inside the droplets, whose conversion range is within the operating region of the gel effect (13). The opacity changes can also be related to the formation of microcrystalline domains in the polymer mass, which can cause scattering of the light.

Regarding the aqueous phase, a gradual change in coloration can be observed up to 35% conversion (16e). This is probably due to the non-negligible solubility of MMA in water (Meyer and Keurentjes, 2005). After that conversion value (35%), changes in the opacity of the aqueous phase are not observed any more. This result may indicate that the MMA solubilized in the aqueous phase polymerize, contradicting some discussions published in the literature (Kalfas et al., 1993). Kalfas et al. (1993) argue that the amount of MMA dissolved in the water does not polymerize and cannot be reabsorbed by the droplets with the evolution of the reaction. Assuming that this is true, then the continuous phase should remain completely transparent throughout the reaction.

One may assume that the amount of monomer dissolved in water can be reabsorbed by the droplets, which would cause the reduction of the opacity, which is not observed. It seems that the small amounts of MMA solubilized (1.58 wt.% Luskin, 1970–1971) in the aqueous phase polymerized and form a nano-dispersion in water, through precipitation. If the system is agitated, then it is possible that the polymer form in the aqueous phase be captured by the larger dispersed droplets.

In order to verify if the Raman monitoring technique could capture the presence of MMA dissolved in the aqueous solution, the aqueous solution of PVA (0.3 wt.%) was saturated with MMA in

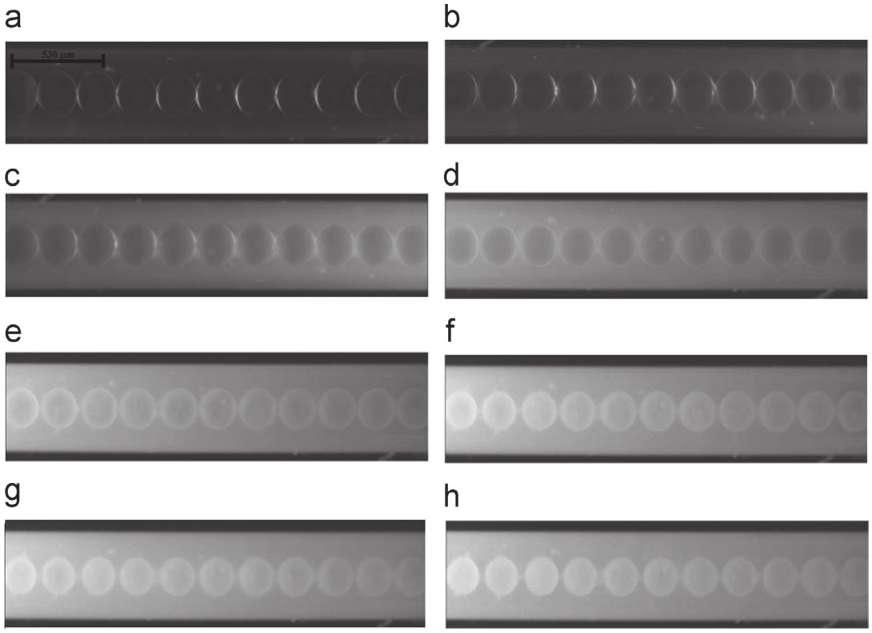

Fig. 16. Evolution of droplets/particles in the suspension polymerization of MMA. Experiment E6. (a) $X=0.2\%$; (b) $X=4.0\%$; (c) $X=7.5\%$; (d) $X=13\%$; (e) $X=35\%$; (f) $X=78.6\%$; (g) $X=86.1\%$; (h) $X=89\%$. Bar length = 530 μm.

the temperature range employed (65–70 °C) and several spectra were obtained. As a result, no significant change was observed in the Raman spectra. Thus, it can be assumed that the proposed Raman technique is not able to monitor the polymerization of the small amounts of monomer dissolved in the aqueous phase. It is important to mention that there is a consensus in the free radical polymerization literature about the fact that the non-negligible solubility of a given monomer in the aqueous phase can cause changes in the suspension polymerization kinetics, when compared with the respective bulk polymerization process (Kalfas et al., 1993; Shan et al., 2004).

In all reactions the spherical shape of the droplets/particles was observed, as shown in Fig. 16. Hence, in order to calculate the volume of the droplets/particles, the volume of a sphere, $\pi d_g^3/6$, was assumed, where d_g is the droplet diameter. The diameter measurements were obtained with the public domain package `ImageJ` 1.48i.

Fig. 17 shows the influence of temperature on the evolution of the particles volume during the polymerization of MMA at a fixed concentration (0.5 wt.%) of the monofunctional initiator LPO in aqueous phase. One can observe that Fig. 17(b) is more representative of the volume changes of the particles, as volumes are reported as functions of conversion.

In order to analyze the variation of droplet size, the percentage change of the droplets was determined, as the initial volumes of all particles could not be kept constant in the experiments. For the reaction conducted at 67.5 °C (E3), a total decrease of volume was equal to 34%, whereas at 70 °C, the total decrease of volume was equal to 30%. It can be stated that these values were similar and compatible with the expected increase of density of the dispersed phase.

Fig. 18 shows the effect of temperature on the volumes of the droplets during the suspension polymerization when using 0.29 wt.% of initiator T141. It can be observed that before the beginning of the gel effect (≈ 35%), large variations of volume take place in both experiments, attaining values of 20.5% and 30% of the initial volume in E6 and E7, respectively. The final volumes of the particles were decreased by 34% and 41% when the temperature was increased from 67.5 °C to 70 °C, respectively. These values were once more compatible with variations expected from density values; although the different values obtained at the different temperatures can also be related to the decrease of particle porosity, caused by the increase of the reaction temperature. This effect is well known in the poly(vinyl chloride) literature (Willmouth et al., 1984; Smallwood, 1986), but has not yet been explored in the PMMA literature.

When one evaluates the effect of increasing the concentration of initiator (T141) on the volume of the droplets in quiescent state, one can observe a smaller decrease of the droplets volume, as shown in Fig. 19. Before the start of the gel effect (≈ 30%), one can

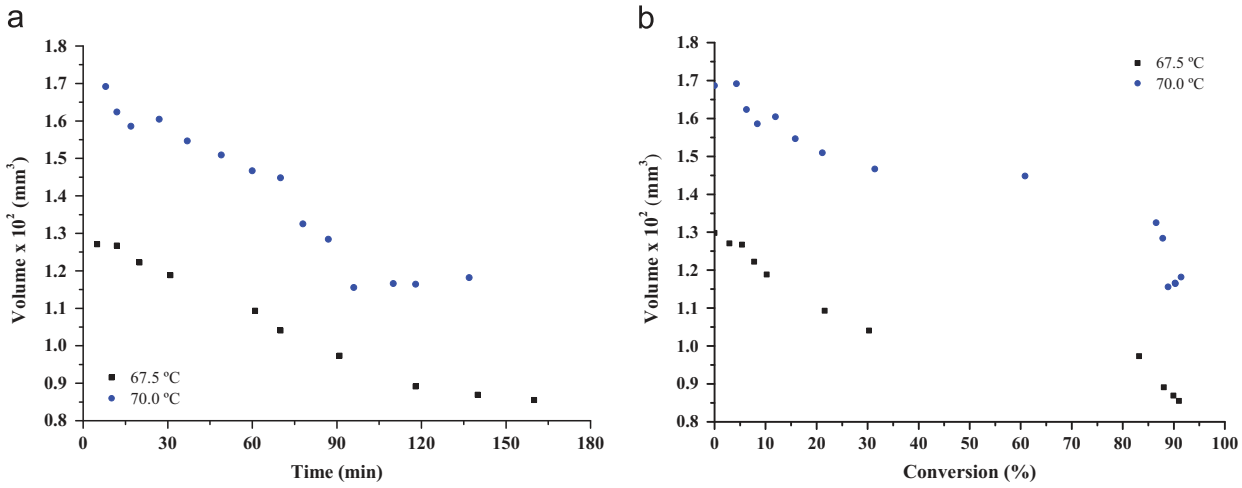

Fig. 17. Temperature effect on the particle volumes during the MMA suspension polymerization. [LPO] = 0.5 wt%; E3 (67.5 °C) and E4 (70 °C). (a) Volume × Time. (b) Volume × Conversion.

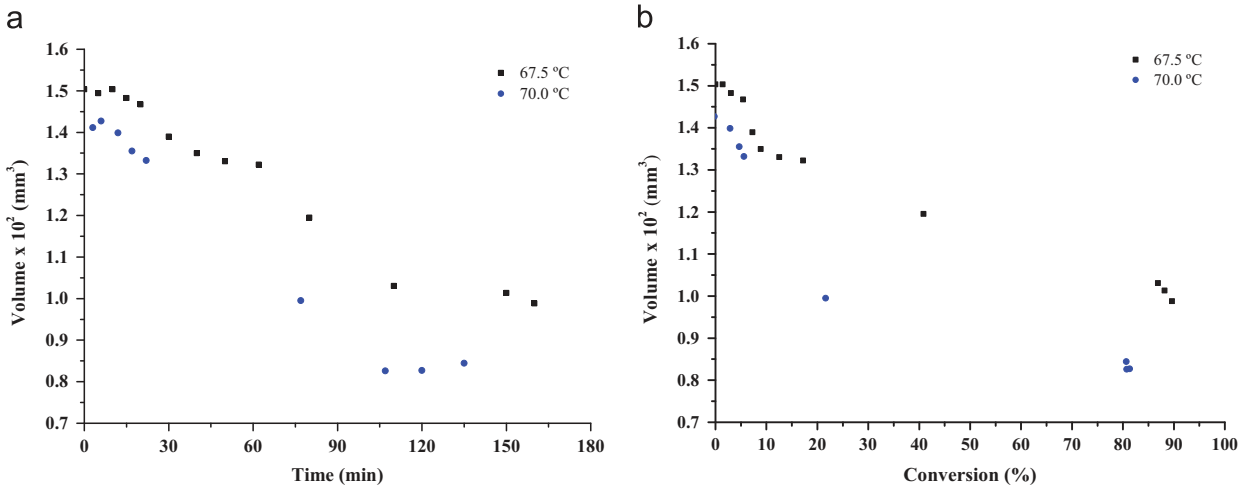

Fig. 18. Temperature effect on particle volumes in MMA suspension polymerizations. [T141] = 0.29 wt%; E6 (67.5 °C) and E7 (70 °C). (a) Volume × Time. (b) Volume × Conversion.

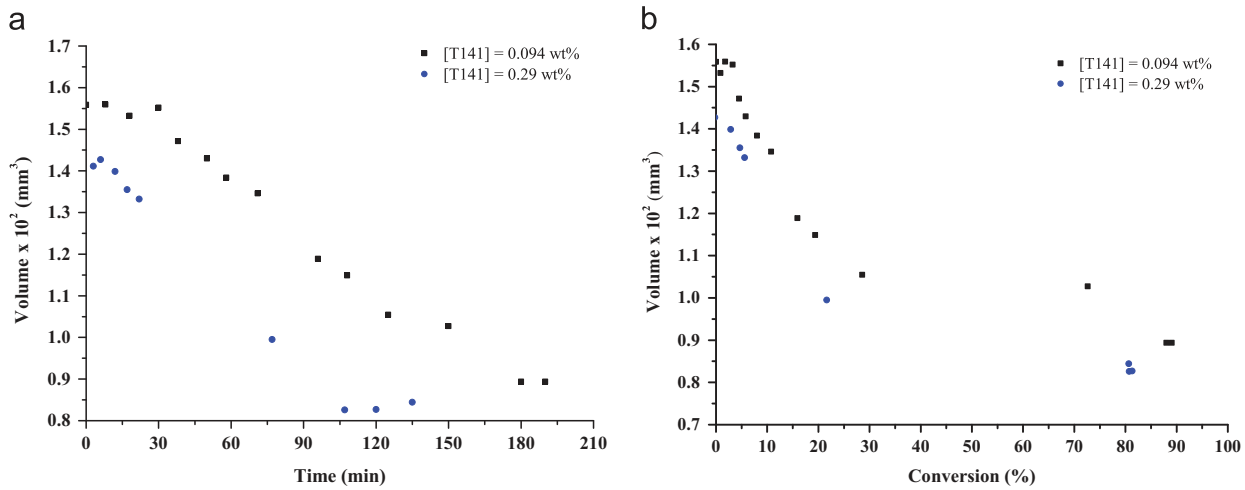

Fig. 19. Effect of the bifunctional initiator concentration on the particle volumes in MMA suspension polymerizations at 70 °C. E7 ([T141]=0.094 wt%) and E8 ([T141]= 0.29 wt%). (a) Volume × Time. (b) Volume × Conversion.

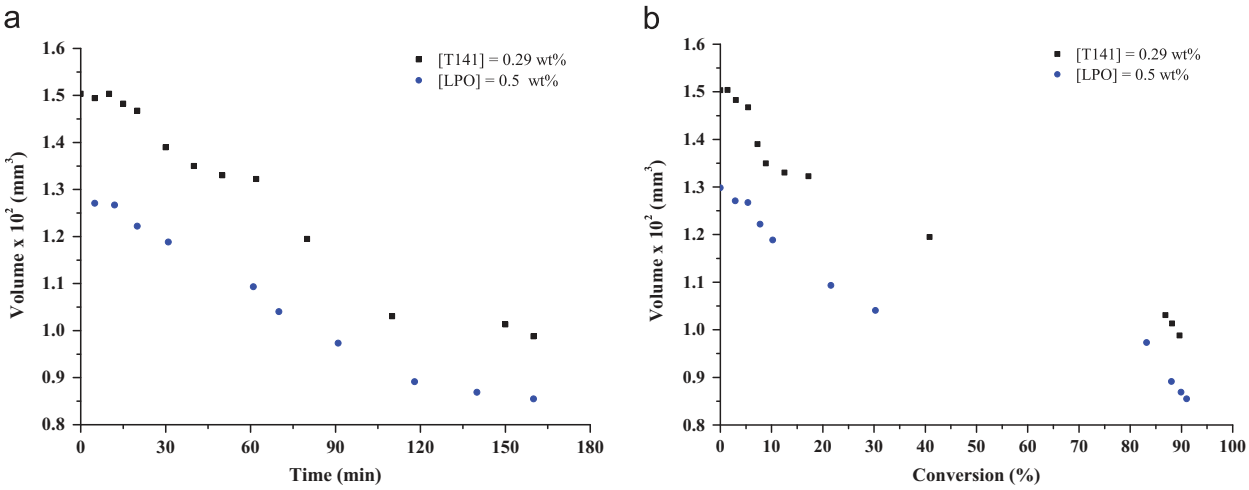

Fig. 20. Evolution of particle volumes in microcapillary at 67.5 °C for reactions performed with the monofunctional ([LPO], E3) and bifunctional ([T141], E6) initiators. (a) Volume × Time. (b) Volume × Conversion.

observe a large variation of the droplets volume in both experiments, which are equal to 30% in E7 and 30.3% in E8, while the total volume decreased 40.8 and 42.6%, respectively. It seems that the temperature exerted a much higher influence on the volume of the particles than the concentration of initiator T141.

The effect of the peroxide initiator on the final size of the particles is shown in Fig. 20. The large decrease of volume observed before 30% of conversion was almost identical, leading to the overall decrease of 34% in volume at the end of the polymerization.

From the results obtained in this section, it can be concluded that the functionality of the initiator and its concentration do not appear to influence significantly the final particle size in the suspension polymerization in quiescent state in microreactors. The reaction temperature seems to exert a much more pronounced effect on the variation of volume, suggesting that both the density and porosity effects may predominate during the volume contraction of the PMMA particles. On the other hand, the results obtained by Jahanzad (2004) in stirred tank reactors indicate that increasing the concentration of the LPO can cause the decrease of the size of the PMMA particles. The author attributed this effect to the balance between the breakage and coalescence rates inside the vessel, controlled by the effect of viscosity of the reacting medium. However, in the absence of effects of breakage and coalescence, there are no reports regarding the effect of initiator type, initiator concentration and reaction temperature on the final particle size of PMMA.

Assuming that the density data presented earlier are representative, then variations of the expected volume should be approximately equal to 18%. As in all experiments, the volume variation of the droplets observed was larger than 18% and these reactions were not subject to the effect of agitation, one can conclude that additional factors seem to dominate these variations, which cannot be explained only in terms of temperature.

A common characteristic observed in all reactions is related to the dynamic profile of the volume change during the formation of PMMA. Based on the available experimental results, where the existence of three stages can be assumed because of the clear change of derivatives of particle volumes (in respect to monomer conversion) observed in most experiments, performed at different reaction conditions, the three characteristic stages during the quiescent state suspension polymerization of MMA in microreactors are:

- `Stage I` (**0**–**35**%): The first stage is characterized by the continuous shrinkage of the MMA droplets, whose volumes can decrease up to 30% of their initial volume. As density changes cannot explain the observed volume changes, it is assumed that MMA polymerization also takes place in the

aqueous phase, with continuous transfer of MMA from particles to the suspending medium.

- `Stage II` (**35–80**%): The second stage is characterized by the small volume change of the droplets, with volume change of approximately 8%. Interestingly, this stage occurs during the highest consumption rate of monomer (gel effect). It seems that occurrence of the gel effect does not modify significantly neither the size nor the morphology of the particles.
- `Stage III` ($>$ **80**%): The third stage is characterized by the identification of the PMMA particles, with volume decrease of approximately 12% in most of the cases presented. This can indicate the slow relaxation of the polymer phase, with slow formation and accommodation of the micro-crystalline polymer material.

4. Conclusions

This work presented a study regarding the implementation of Raman spectroscopic technique for monitoring of the suspension polymerization of MMA in microreactors. Raman spectroscopy was shown to be sensitive to the usual variations of the most important process variables, such as the initiator type, initiator concentration and the reaction temperature. It was also shown that the choice of an adequate internal reference allowed for the successful monitoring of the monomer conversion with the proposed Raman technique.

The kinetic data obtained in the present study were compatible with kinetic data reported in the literature for MMA polymerizations. Particularly, the performances of a bifunctional initiator (T141) with a monofunctional initiator (LPO) were compared to each other, showing that the initiator T141 produces higher reaction rates, higher average molar mass and lower dispersity.

It was also possible to relate the reaction kinetics with the evolution of the volume of droplets during the MMA polymerization. For the first time, stages of evolution of the volume of the droplets/particles of MMA/PMMA were reported, according to monomer conversion for suspension polymerization in the absence of breakage and coalescence effects. It was observed that the morphological evolution of the droplets is probably affected by the reactions in the aqueous phase, which can be explained by the low partial solubility of MMA in water. It was shown that the volume changes of the drops were not functions only of the conversion and that other significant effects can affect the droplet/particle volume in a broad range of conversion.

Acknowledgments

The authors thank CNPq (Conselho Nacional de Desenvolvimento Científico e Tecnológico, Brazil) for scholarships and financial support. The authors also thank ENSIACET (École Nationale Supérieure des Ingénieurs en Arts Chimiques et Technologiques) and CNRS (Centre National de la Recherche Scientifique) for financial support.

References

Bally, F., Serra, C.A., Hessel, V., Hadziioannou, G., 2010. Homogeneous polymerization: benefits brought by microprocess technologies to the synthesis and production of polymers. Macromol. React. Eng. 4 (9–10), 543–561.

Barnes, S.E., Cygan, Z.T., Yates, J.K., Beers, K.L., Amis, E.J., 2006. Raman spectroscopic monitoring of droplet polymerization in a microfluidic device. Analyst 131 (9), 1027–1033.

Bayer, T., Pysall, D., Wachsen, O., 2000. Microreaction Technology: Industrial Prospects. No. 4. Springer Berlin Heidelberg, Berlin, Ch. Micro mixing effects in continuous radical polymerization. In: IMRET 3: Proceedings of the Third International Conference on Microreaction Technology, pp. 165–170.

Benbachir, M., Benjelloun, D., 2001. Investigation of free radical polymerization using diperoxyesters as bifunctional initiators. Polymer 42 (18), 7727–7738.

Benson, R.S., Ponton, J.W., 1993. Process miniaturization—a route to total environmental acceptability? Trans. Ind. Chem. Eng. 71 (A2), 160–168.

Bodoc, M.D., Prat, L., Xuereb, C., Gourdon, C., Lasuye, T., 2012. Online monitoring of vinyl chloride polymerization in a microreactor using Raman spectroscopy. Chem. Eng. Technol. 35 (4), 705–712.

Brandrup, J., Immergut, E.H., Grulke, E.A., Abe, A., Bloch, D.R., 1999. 4th ed.Polymer Handbook, vol. 2. John Wiley & Sons, Canada.

Cabral, J., Hudson, S., Wu, T., Beers, K., Douglas, J., 2004. Microfluidic combinatorial polymer research. Polym. Mater.: Sci. Eng. 90, 337–338.

Cavin, L., Rouge, A., Meyer, T., Renken, A., 2000. Kinetic modeling of free radical polymerization of styrene initiated by the bifunctional initiator 2,5-dimethyl-2,5-bis(2-ethyl hexanoylperoxy)hexane. Polymer 41, 3925–3935.

Chang, Z., Liu, G., Fang, F., Tian, Y., Zhang, Z., 2004. gamma-ray-initiated dispersion polymerization of pma in microreactor. Chem. Eng. J. 101 (1–3), 195–199.

Chu, B., Lee, D.-C., 1984. Characterization of poly(methyl methacrylate) during the thermal polymerization of methyl methacrylate. Macromolecules 17 (4), 926–937.

Edwards, H., Johal, K., Johnson, A., 2006. Ft-raman spectroscopic monitoring of the group-transfer polymerisation of methyl methacrylate. Vib. Spectrosc. 41, 160–169.

Ehrfeld, W., Hessel, V., Löwe, H., 2000. Extending the knowledge base in microfabrication towards chemical engineering and fluid dynamic simulation In: AIChE (Ed.), 4th International Conference on Microreaction Technology: Topical Conference Proceedings. vol. IMRET 4. Atlanta, p. 3.

Feng, L., Ng, K.S., 1991. Characterization of styrene polymerization in microemulsions by Raman spectroscopy. Colloids Surf. 53 (2), 349–361.

Fernandes, P., 2010. Miniaturization in biocatalysis. Int. J. Mol. Sci. 11 (3), 858–879.

Gulari, E., McKeigue, K., Ng, K.Y.S., 1984. Raman and FTIR spectroscopy of polymerization: bulk polymerization of methyl methacrylate and styrene. Macromolecules 17 (9), 1822–1825.

Hagan, C.P., Orr, J.F., Mitchell, C.A., Dunne, N.J., 2009. Real time monitoring of the polymerisation of pmma bone cement using Raman spectroscopy. J. Mater. Sci.: Mater. Med. 20, 2427–2431.

Honda, T., Miyazaki, M., Nakamuraa, H., Maeda, H., 2005. Controllable polymerization of n-carboxy anhydrides in a microreaction system. Lab Chip 5 (8), 812–818.

Iwasaki, T., Kawano, N., Yoshida, J.-I., 2006. Radical polymerization using microflow system: numbering-up of microreactors and continuous operation. Org. Process Res. Dev. 10 (6), 1126–1131.

Iwasaki, T., Yoshida, J., 2005. Free radical polymerization in microreactors. significant improvement in molecular weight distribution control. Macromolecules 38 (4), 1159–1163.

Jahanzad, F., 2004. Evolution of Particle Size Distribution in Suspension Polymerization Reactions (Ph.D. thesis), Loughborough University, Loughborough, England.

Jensen, K.F., 2001. Microreaction engineering—is small better? Chem. Eng. Sci. 56 (2), 293–303.

Jeong, W.J., Kim, J.Y., Choo, J., Lee, E.K., Han, C.S., Beebe, D.J., Seong, G.H., Lee, S.H., 2005. Continuous fabrication of biocatalyst immobilized microparticles using photopolymerization and immiscible liquids in microfluidic systems. Langmuir 21 (9), 3738–3741.

Kalfas, G., Yuan, H., Ray, W.H., 1993. Modeling and experimental studies of aqueous suspension polymerization processes. 2. Experiments in batch reactors. Ind. Eng. Chem. Res. 32 (9), 1831–1838.

Kang, L., Chung, B., Langer, R., Khademhosseini, A., 2008. Microfluidics for drug discovery and development: from target selection to product lifecycle management. Drug Discov. Today 1, 1–13.

Kiwi-Minsker, L., Renken, A., 2005. Microstructured reactors for catalytic reactions. Catal. Today 110, 2–14.

Koenig, J.L., 1999. Spectroscopy of Polymers, 2nd edition Elsevier, New York.

Koenig, J.L., 2001. Infrared and Raman Spectroscopy of Polymers, vol. 12. Rapra Review Report, UK.

LaVision, 2006. DaVis StrainMaster Software Manual 7.1. GmbH, Alemanha, Gottingen.

Lerou, J.J., Harold, M.P., Ryley, J., O'Brien, J.A.T.C., Johnson, M., Perrotto, J., Blaisdell, C.T., Rensi, T.A., Nyquist, J., 1996. Microfabricated minichemical systems: technical feasibility. In: Ehrfeld, W. (Ed.), Microsystem Technology for Chemical and Biological Microreactors, vol. 132. DECHEMA Monographs, Verlag Chemie, pp. 51–69.

Lipiecki, F., Maroldo, S., Shenai-Khatkhate, D.V., Ware, R.A., 2008. Purification process using microchannel devices. PATENT US-12/215,827.

Lipiecki, F., Maroldo, S., Shenai-Khatkhate, D.V., Ware, R.A., 2009. Method of preparing organometallic compounds using microchannel devices. PATENT US-20090023940 A1.

Liu, Z., Lu, Y., Yang, B., Luo, G., 2011. Controllable preparation of poly(butyl acrylate) by suspension polymerization in a coaxial capillary microreactor. Ind. Eng. Chem. Res. 50 (21), 11853–11862.

Lorber, N., Pavageau, B., Mignard, E., 2010. Investigating acrylic acid polymerization by using a droplet-based millifluidics approach. Macromol. Symp. 296, 203–209.

Luskin, L.S., 1970–1971. In Vinyl and Diene Monomers, wiley-interscience Edition. Vol. 1. John Wiley & Sons, New York, Ch. Acrylic Acid, Methacrylic Acid, and the Related Eaters, pp. 105–203.

Massignani, M., Lomas, H., Battaglia, G., 2010. Modern Techniques for Nano- and Microreactors/-reactions. Vol. 229. Springer Berlin Heidelberg,

Ch. Polymersomes: A Synthetic Biological Approach to Encapsulation and Delivery, pp. 115–154.
McCreery, R.L., 2000. Raman Spectroscopy for Chemical Analysis, vol. 157. John Wiley & Sons, New York.
Meyer, T., Keurentjes, J., 2005. Handbook of Polymer Reaction Engineering, 1st ed. WILEY-VCH Verlag GmbH & Co, Weinheim.
Nagaki, A., Kawamura, K., Suga, S., Ando, T., Sawamoto, M., Yoshida, J.-I., 2004. Cation pool-initiated controlled/living polymerization using microsystems. J. Am. Chem. Soc. 126 (45), 14702–14703.
Nielsen, C.A., Chrisman, R.W., LaPointe, R.E., Jr., Miller, T.E. 2002. Novel tubing microreactor for monitoring chemical reactions. Anal. Chem. 74 (13), 3112–3117.
Nisisako, T., Torii, T., Higuchi, T., 2004. Novel microreactors for functional polymer beads. Chem. Eng. J. 101 (1), 23–29.
Nobel, A., 2008. Product Data Sheet. Akzo Nobel, Holanda.
Odian, G., 2004. Principles of Polymerization, 4th ed. John Wiley and Sons Inc., New York, EUA.
Pattekar, A., Kothare, M., 2004. A microreactor for hydrogen production in micro fuel cell applications. J. Microelectromech. Syst. 13 (1), 7–18.
Pelletier, M.J., 1999. Effects of temperature on cyclohexane raman bands. Appl. Spectrosc. 53 (9), 1087–1096.
Richard, R., Dubreuil, B., Thiebaud-Roux, S., Prat, L., 2013. On-line monitoring of the transesterification reaction carried out in microreactors using near infrared spectroscopy. Fuel 104, 318–325.
Russum, J.P., Jones, C.W., Schork, F.J., 2004. Continuous reversible addition-fragmentation chain transfer polymerization in miniemulsion utilizing a multi-tube reaction system. Macromol. Rapid Commun. 25 (11), 1064–1068.
Salic, A., Tusek, A., Zelic, B., 2012. Application of microreactors in medicine and biomedicine. J. Appl. Biomed. 10, 137–153.
Scorah, M.J., Cosentino, R., Dhib, R., Penlidis, A., 2006. Experimental study of a tetrafunctional peroxide initiator: bulk free radical polymerization of butyl acrylate and vinyl acetate. Polym. Bull. 51, 157–167.
Scorah, M.J., Dhib, R., Penlidis, A., 2004. Free-radical polymerization of methyl methacrylate with a tetrafunctional peroxide initiator. J. Polym. Sci.: Part A: Polym. Chem. 42, 5647–5661.
Shan, G., Li, J., Huang, Z., Weng, Z., Lu, Q., 2004. Effects of water solubility of monomer on the kinetics of methyl methacrylate suspension polymerization. Acta Polym. Sin. 1 (1), 121–124.
Sheng, W., Shan, G.-R., Huang, Z.-M., Weng, Z.-X., Pan, Z., 2005. Decomposition of 2,5-dimethyl-2,5-di(2-ethylhexanoyl -peroxy)hexane and its use in polymerization of styrene and methyl methacrylate. Polymer 46 (23), 10553–10560.
Smallwood, P.V., 1986. The formation of grains of suspension poly(vinyl chloride). Polymer 27 (10), 1609–1618.
Sotowa, K.-I., Sueyoshi, Y., Kusakabe, K., 2004. Copolymerization of styrene and methyl methaerylate in a microchannel. Kagaku Kogaku Ronbunshu 30 (2), 117–121.
Sun, J., Ju, J., Ji, L., Zhang, L., Xu, N., 2008. Synthesis of biodiesel in capillary microreactors. Ind. Eng. Chem. Res. 47 (5), 1398–1403.
Van, M., Brink, D., Hansen, J.-F., Peinder, P., Herk, A.M.V., German, A.L., 2001. Measurement of partial conversions during the solution copolymerization of styrene and butyl acrylate using on-line Raman spectroscopy. J. Appl. Polym. Sci. 79 (3), 426–436.
Wang, C., Vickers, T., Schlenoff, J., Mann, C., 1992. In situ monitoring of emulsion polymerization using fiber-optic Raman spectroscopy. Appl. Spectrosc. 46 (11), 1729–1731.
Wegeng, R.W., Call, C.J., Drost, M.K., 1996. Chemical system miniaturization. In: Proceedings of the AIChE Spring National Meeting. New Orleans, pp. 1–13.
Willis, H.A., Zichy, V.J.I., Hendra, P.J., 1969. The laser-raman and infra-red spectra of poly(methyl methacrylate). Polymer 10, 737–746.
Willmouth, F.M., Rance, D.G., Henman, K.M., 1984. An investigation of precipitation polymerization in liquid vinyl chloride by photon correlation spectroscopy. Polymer 25 (8), 1185–1192.
Wu, T., Mei, Y., Cabral, J.T., Xu, C., Beers, K.L., 2004. A new synthetic method for controlled polymerization using a microfluidic system. J. Am. Chem. Soc. 126 (32), 9880–9881.
Xie, S., Iglesia, E., Bel, A., 2001. Effects of temperature on the Raman spectra and dispersed oxides. J. Phys. Chem. B 105, 5144–5152.
Yadav, A.K., Krell, M., Hergeth, W.-D., de la Cal, J.C., Barandiaran, M.J., 2014. Monitoring polymerization kinetics in microreactors by confocal raman microscopy. Macromol. React. Eng. 8, 543–549.
Yoon, W.J., Choi, K.Y., 1992. Free radical polymerization of styrene with a binary mixture of symmetrical bifunctional initiators. J. Appl. Polym. Sci. 46, 1353–1367.
Zhang, X., Stefanick, S., Villani, F.J., 2004. Application of microreactor technology in process development. Org. Process Res. Dev. 8, 455–460.